

Ginga observations of the old nova GK Persei in quiescence and outburst

M. Ishida,¹ T. Sakao,¹★ K. Makishima,¹ T. Ohashi,¹ M. G. Watson,² A. J. Norton,³
M. Kawada⁴ and K. Koyama⁴†

¹Department of Physics, Faculty of Science, University of Tokyo, 7-3-1, Hongo, Bunkyo-ku, Tokyo 113, Japan

²X-ray Astronomy Group, Department of Physics and Astronomy, University of Leicester, University Road, Leicester LE1 7RH

³High-Energy Astrophysics Group, Physics Department, University of Southampton, Southampton, Hampshire SO9 5NH

⁴Department of Astrophysics, School of Science, Nagoya University, Furo-cho, Chikusa-ku, Nagoya 464-01, Japan

Accepted 1991 September 18. Received 1991 September 16; in original form 1991 August 19

SUMMARY

We report *Ginga* observations of the old nova GK Persei in quiescence, as well as a brief scanning observation during an outburst. The X-ray spectrum in quiescence is well fitted by thermal bremsstrahlung emission of very high temperature ($kT \sim 30$ keV), plus an iron emission line. In contrast, the outburst spectrum is complex and comprises two continua with different column densities ($N_{\text{H}} \sim 10^{23}$ and $\sim 10^{24}$ cm⁻²). The 351-s spin modulation of GK Per was clearly detected in the quiescence observation, which confirms the results of previous *EXOSAT* observations. The folded light curve shows two peaks that are not separated by 180° in phase, which is indeed quite different from the *EXOSAT* outburst data. It is, however, similar to the *EXOSAT* observation at a similar flux level.

1 INTRODUCTION

The old nova GK Per (Nova Per 1901) is an X-ray emitting cataclysmic variable with an orbital period of 48 hr (Crampton, Cowley & Hutchings 1983), containing a white dwarf which accretes mass from a somewhat evolved (K2IV) companion star (Warner 1976). Roughly every ~ 400 d, GK Per exhibits optical outbursts lasting for 50–100 d (Hudec 1981). The outbursts involve optical brightening by 1–3 visual magnitudes and a ten-fold intensity increase in X-rays (King, Ricketts & Warwick 1979; Becker & Marshall 1981; Cordova & Mason 1984). The *EXOSAT* observations of GK Per during an outburst in 1983 August led to the discovery of the spin period of 351 s, with the X-ray modulation amplitude of more than 50 per cent in the 3–11 keV energy band (Watson, King & Osborne 1985; hereafter WKO85). Subsequent *EXOSAT* observations in quiescence (1984 September 2–3 and 1985 January 9–10) revealed interesting changes in the X-ray spectrum as well as in the pulse profiles (Norton, Watson & King 1988; hereafter NWK88).

We here report on X-ray observations of GK Per made in 1987 September using the Large Area Proportional Counter (LAC) on board *Ginga*. Although the old nova was in quiescence, the large effective area and the high sensitivity of the LAC enabled us to obtain a high-quality energy spectrum, especially above 10 keV, and to detect the spin period. We

also report on a brief scanning observation of GK Per made with the LAC in 1989 September during an optical outburst. These results confirm, and further extend, our knowledge of X-ray emission from GK Per.

2 OBSERVATIONS

2.1 Pointed observations in quiescence

We observed GK Per on 1987 September 22–24 using the Large Area Proportional Counter (LAC) on board *Ginga*. The LAC consists of eight gas proportional counters with a total effective area of 4000 cm² (Turner *et al.* 1989). During the observations, X-ray data were taken in the MPC-2 mode with low bit-rate, in which 1.2–37 keV spectra are acquired every 2 s in 48 spectral channels. The background observation was performed before the on-source observation, on 1987 September 21.

Fig. 1 is the light curve of GK Per during these observations in three energy ranges, 1.2–4.7, 4.7–9.3, and 9.3–18.6 keV. The background was subtracted using the ‘SUD-sorting’ method (Hayashida *et al.* 1989). The average source flux was ~ 9 count s⁻¹ in the 1.2–9.3 keV band, or ~ 1 mCrab, which is close to that of ‘observation E’ reported in NWK88. The light curve shows significant flickering.

2.2 Scanning observations in outburst

GK Per was observed again with the LAC on 1989 September 7 during a single scan which was performed as a part of an X-ray survey over the Perseus region. The source

★ Present address: National Astronomical Observatory of Japan, Osawa, Mitaka, Tokyo 181, Japan.

† Present address: Department of Physics, Kyoto University, Sakyo-ku, Kyoto 606, Japan.

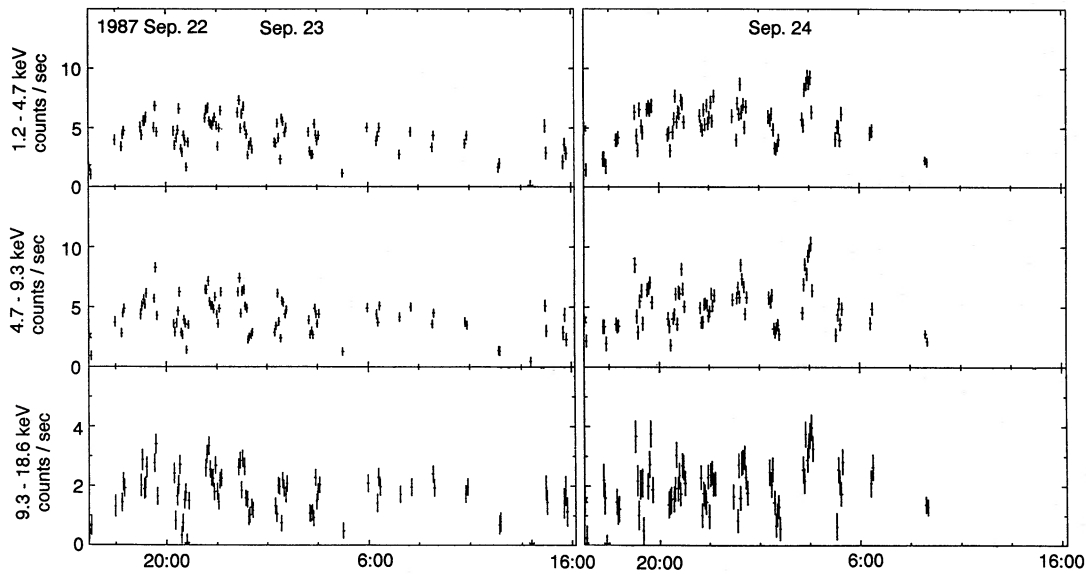


Figure 1. The background-subtracted X-ray light curves of GK Per from the pointed observations in 1989 September, displayed in three energy bands (1.2–4.7, 4.7–9.3 and 9.3–18.6 keV). Each point is the average of 256 s.

was in a late stage of a moderate optical outburst which had started in 1989 July (*IAU Circulars* 4819, 4827, 4831, 4855). Fig. 2 shows the X-ray light curve as a function of scan angle, where GK Per is seen as a clear peak in addition to a softer peak due to the Perseus cluster. As GK Per passed ~ 1.3 from the centre of the LAC field of view, the peak transmission of the LAC collimator ($2^\circ \times 1^\circ$ FWHM) for GK Per was about 40 per cent. Correction for this efficiency gave the 1.2–9.3 keV intensity of 90 count s^{-1} . This is ~ 10 times higher than that obtained in the pointed observations in quiescence, and corresponds to about 70 per cent of the *EXOSAT* outburst flux (WKO85).

3 DATA ANALYSIS AND RESULTS

3.1 X-ray pulse-height spectrum

We summed all the pointed data into a single pulse-height spectrum. Fig. 3(a) shows the ‘quiescence’ spectrum thus obtained, together with the ‘outburst’ spectrum, derived from the scanning data after proper aspect correction. In spite of the higher source intensity, the outburst spectrum is of poorer quality than the quiescent spectrum because of the much shorter effective exposure time (~ 100 s). Both spectra are very hard and show an iron *K* emission-line feature at 6–7 keV. In Fig. 3(b) we present channel-by-channel ratios between the two spectra. The outburst spectrum is significantly more absorbed than the other, with a clear iron *K*-edge absorption structure at ~ 8 keV as well as a more prominent iron emission line. These differences between the two spectra agree qualitatively with the *EXOSAT* results (WKO85; NWK88), and can be attributed to a larger amount of accreting matter around the white dwarf during the outburst.

3.2 Parameters for the quiescent spectrum

We fitted the observed quiescent spectrum with a thermal bremsstrahlung continuum together with photoelectric

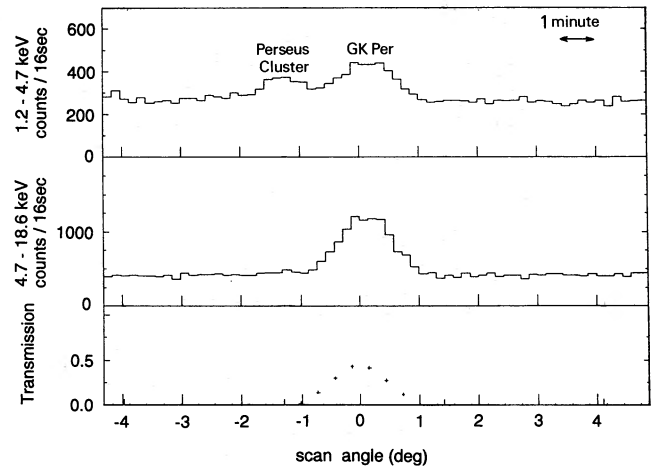


Figure 2. Background-inclusive X-ray scan profiles of the Perseus region obtained on 1989 September 7, UT 9:53 to 10:12. The upper two profiles correspond to 1.2–4.7 and 4.7–18 keV, while the bottom trace gives the expected collimator transmission to GK Per. The length of the arrow in the top panel indicates 1 min.

absorption [using the cross-section by Morrison & McCammon (1983), which includes effects up to the iron *K*-shell], plus a narrow (0.1-keV FWHM) Gaussian component representing the iron line. As shown in Fig. 4(a) (by solid histograms) and Table 1, this model gave an acceptable fit to the data. Fig. 5(a) shows two-parameter confidence contours for the bremsstrahlung temperature kT versus hydrogen column density N_{H} , while Fig. 5(b) gives that for the iron line centre energy versus iron line intensity. We have thus detected the iron line from GK Per in quiescence for the first time. The implied temperature is confined to the range of 25–42 keV at the 90 per cent confidence level. These values are consistent with that obtained in the *EXOSAT* ‘observation D’ (NWK88). The absorbing column, $N_{\text{H}} \sim 10^{22} \text{ cm}^{-2}$, is about three times smaller than those from the *EXOSAT*

observations in quiescence. Because the spectrum is very hard, a power-law continuum instead of thermal bremsstrahlung gives a similarly good fit ($\chi^2_\nu = 0.88$; best-fitting photon index = 1.55 ± 0.06).

3.3 Parameters for the outburst spectrum

We have also attempted to fit the outburst spectrum with a thermal bremsstrahlung with low-energy absorption plus a narrow line. The results are listed in Table 1 and shown in Fig. 4(b). A power-law continuum fit was also tried. The power-law fit gives almost the same value of χ^2_ν with a photon index ~ 1.2 , but these fits are formally unacceptable, mainly due to negative residuals at 7–8 keV. This suggests that the iron *K*-edge feature in the outburst spectrum is apparently deeper than is implied by the low-energy (< 5 keV) absorption. Similar phenomena have often been observed from X-ray pulsars (e.g. Nagase 1989) and active galactic nuclei (Pounds *et al.* 1990). We recall that the *EXOSAT* continuum spectrum of GK Per in outburst was also too complex to be represented by a single continuum with absorption (WKO85).

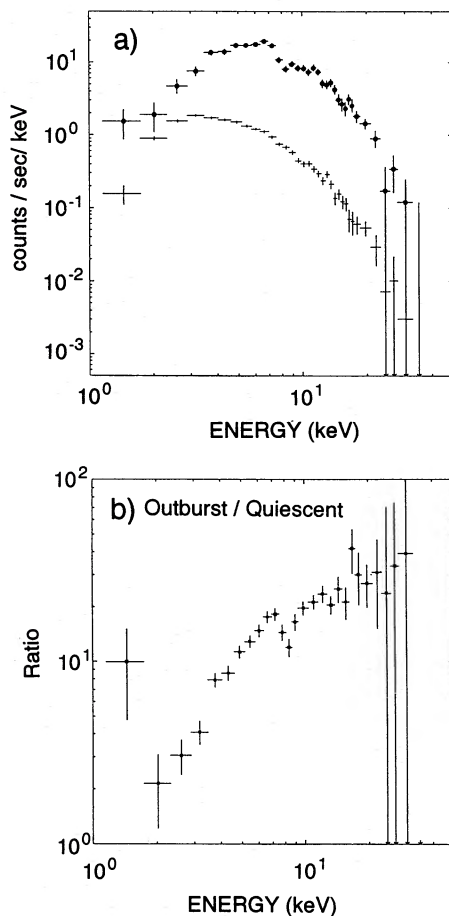


Figure 3. (a) X-ray pulse-height spectra of GK Per, after aspect correction and background subtraction. Crosses represent the quiescent spectrum from the pointed observations with an effective exposure of 20 100 s, while data with filled circles show the outburst spectrum derived from the scanning data. Both spectra include the instrumental response. (b) The channel-by-channel ratios of the two pulse-height spectra.

The fit may be improved by assuming one of the following: (i) the effective low-energy absorption is reduced due to substantial ionization of the absorbing matter ('warm absorber' model); (ii) absorbing matter exhibits a significant distribution in column density ('leaky absorber' model; Norton & Watson 1989); (iii) the low-energy absorption is masked by a separate soft component ('soft excess' model; WKO85), or (iv) the low-energy absorption is masked by a soft component generated by Compton degradation of the primary component (Illarionov & Sunyaev 1972; Kylafis & Lamb 1979, 1982). In spectral fitting, the first case can be examined by allowing column densities for the low-energy absorption (N_H) and iron *K*-edge absorption (N_{Fe}) to vary independently. The other three cases are tested by introducing another thin thermal component whose temperature, N_H and normalization are treated as free parameters, though, in the second case, the temperature is set to be the same as that of the primary component. As before, we take a thin thermal spectrum as a primary component. We also include a Gaussian line for all four models.

Table 2 summarizes the results of fittings for the first two cases. While the warm absorber model is not fully successful, the leaky absorber model has attained an acceptable fit. In Fig. 4(c) we present the fit with the 'leaky absorber' model. When we remove the equi-temperature restriction of the two components, a minimum chi-square value of 1.1 is obtained for continuum parameters of $kT_S = 3$ keV with $\log N_H = 23.1$, and $kT_H = 27$ keV with $\log N_H = 23.9$ (soft excess model), where kT_S and kT_H are the temperature of the soft component and the hard component respectively. Alternatively, a similarly good fit ($\chi^2_\nu = 1.2$) is obtained for $kT_S = 13$ keV with $\log N_H = 24.3$, and $kT_H = 29$ keV with $\log N_H = 22.9$ (Compton degradation model). However, the error regions of two temperatures overlap at the 90 per cent confidence level for both cases, whereas the typical error of $\log N_H$ is of order ~ 0.1 . So the difference in column densities between the two components is significant.

We conclude that at least two continuum components are required to explain the outburst spectrum; one absorbed with $N_H \sim 10^{23} \text{ cm}^{-2}$ corresponding to the low-energy absorption, and the other with $N_H \sim 10^{24} \text{ cm}^{-2}$ in accordance with the iron *K*-edge depth. These are similar to the *EXOSAT* results. The two column density model also applies to other intermediate polars observed with *EXOSAT* (Norton & Watson 1989), and FO Aqr observed with *Ginga* (Norton *et al.* 1990). We remark that the absorbing matter may have a continuous distribution instead of two representative column densities, as discussed by Norton, Watson & King (1991). We cannot, however, decide whether the two components have different temperatures or not. Considering the ambiguities in the correct model, the bremsstrahlung temperature obtained cannot be distinguished from that for the quiescent spectrum.

3.4 Pulse period and modulation light curve

Using the quiescence data spanning two days, we performed a standard folding analysis and unambiguously confirmed the 351-s periodicity. The pulse period which maximized the reduced chi-squared turned out to be 351.3 ± 0.1 s, in good agreement with the *EXOSAT* results (WKO85; NWK88). Note that the expected orbital Doppler effect of GK Per does

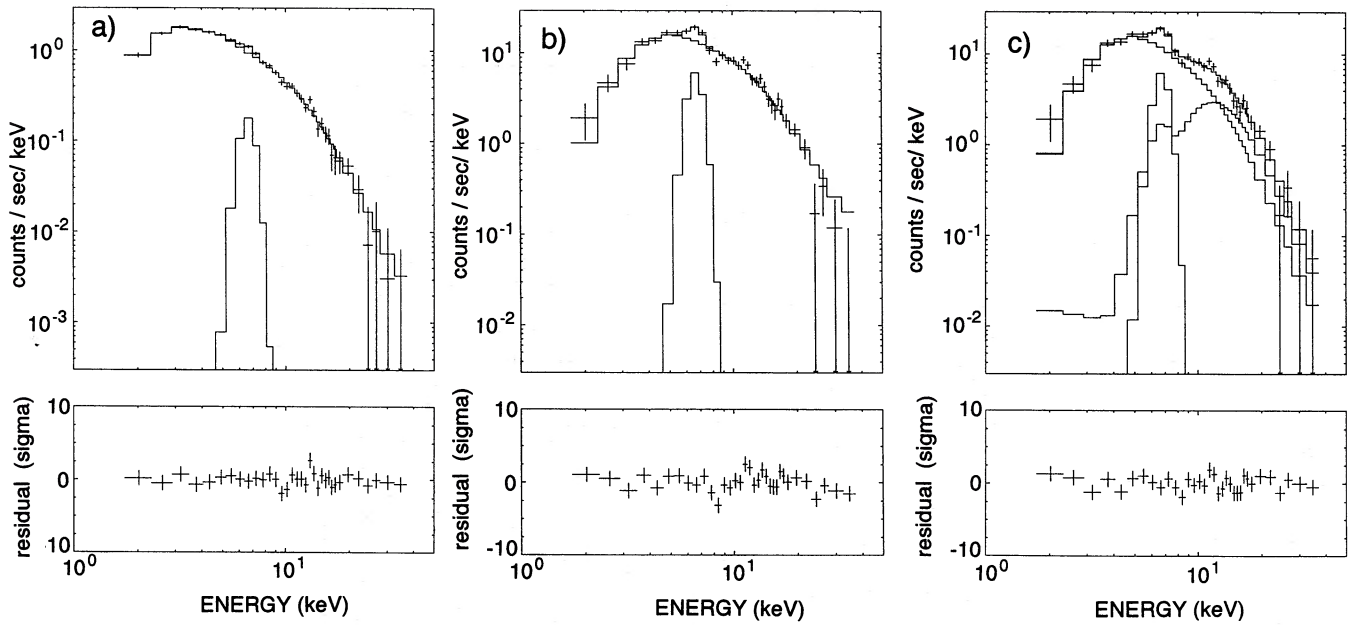


Figure 4. Results of model fitting to the observed spectra. Upper panels show the best-fitting model (histograms) convolved through the detector response, to be compared with the data. Lower panels show the fit residuals. (a) The quiescent spectrum, fitted with a single bremsstrahlung continuum with absorption, plus a Gaussian emission line (see Table 1). (b) The same as (a), but for the outburst spectrum (see Table 1). (c) The outburst spectrum fitted with the leaky absorber model (see text and Table 2).

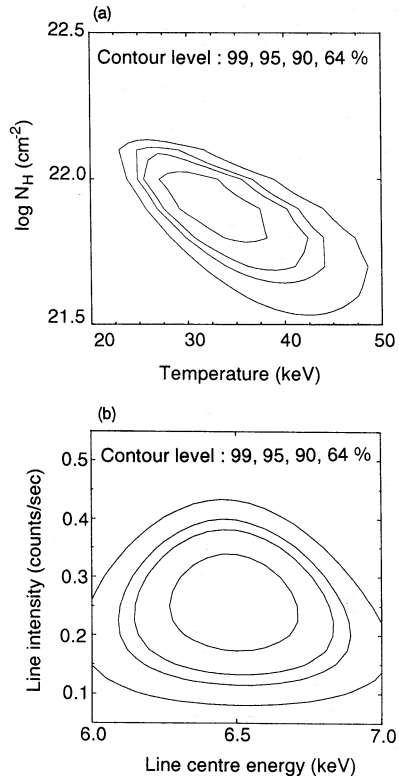


Figure 5. Confidence contours of fitted parameters for the quiescent spectrum using a model composed of a thermal bremsstrahlung continuum with low-energy absorption plus iron line (see text and Table 1). Contour levels are 99, 95, 90 and 64 per cent. Details of each panel are: (a) Photoelectric absorbing column N_{H} versus continuum temperature kT (for the quiescent spectrum). (b) Iron line intensity versus line centre energy (for the quiescent spectrum).

not affect the spin period by more than ± 0.02 s, which is within the observational uncertainty. Figs 6(a) and (b) show the chi-squared behaviour and the modulation light curve, respectively. The folded light curve shows a two-peak structure, reminiscent of the results from the *EXOSAT* ‘observation E’ (NWK88). Since the pulse modulation is rather small (≤ 20 per cent), the flickering behaviour seen in Fig. 1 is mostly unrelated to the 351-s modulation. We could not study the pulsation during the outburst scanning observation, because the effective exposure time was too short (~ 100 s).

The spin-folded light curves are characterized by a larger modulation amplitude in lower energy bands. The softness ratio is also modulated and suggests a relatively softer energy spectrum at the pulse maximum than at the pulse minimum. Similar characteristics were observed in outburst (WKO85). In Fig. 7, we show the measured modulation amplitude as a function of X-ray energy in comparison with that in outburst taken from WKO85. Indeed, the outburst data show similar tendency to the quiescent data though the amplitude is larger by a factor of ~ 4 . In order to examine this property further, we have constructed a pulse-minimum spectrum ($\phi = 0.00\text{--}0.16$ and $0.84\text{--}1.00$ in Fig. 6b) and a pulse-maximum spectrum ($\phi = 0.16\text{--}0.84$), and fitted them with the same single thermal bremsstrahlung with low-energy absorption and an iron line. Fig. 8 shows the confidence contours of these spectra in the $kT\text{--}N_{\text{H}}$ plane. It is likely that only N_{H} is modulated. We have therefore tried to fit both spectra with the temperature fixed at 32 keV, which is the value of the phase-average spectrum. The results are listed in Table 1. Normalizations of the continua are the same within the errors in both spectra. These results demonstrate that the spin modulation of GK Per in quiescence is mostly caused by the variation of the low-energy absorption.

Table 1. Single thermal bremsstrahlung fits to the spectra.

	Quiescent			Outburst
	average	pulse-maximum	pulse-minimum	
Bremsstrahlung continuum				
norm.				
(10^{-2} photon $s^{-1}cm^{-2}keV^{-1}$)	0.39 ± 0.02	0.39 ± 0.01	0.38 ± 0.01	5.3 ± 1.9
temperature (keV)	32_{-7}^{+10}	32^b	32^b	> 42
$\log N_H(cm^{-2})$	22.0 ± 0.2	21.9 ± 0.1	22.2 ± 0.1	22.9 ± 0.1
Iron Line				
centre energy (keV)	6.5 ± 0.2	6.4 ± 0.2	6.8 ± 0.2	6.6 ± 0.2
flux (10^{-4} photon $s^{-1}cm^{-2}$)	0.65 ± 0.24	0.64 ± 0.25	0.77 ± 0.29	25 ± 7
equivalent width (eV)	250 ± 150			790 ± 250
2-20 keV flux ($10^{-11}erg s^{-1}cm^{-2}$) ^c	4.0 ± 0.4			48 ± 17
2-20 keV luminosity ($10^{33}erg s^{-1}$) ^d	1.3 ± 0.1			16 ± 6
χ^2/ν	0.74	0.61	0.88	1.63
degrees of freedom	29	30	30	29

^aQuoted errors refer to single-parameter 90 per cent confidence limits.

^bFixed at the value obtained from the fit to the average spectrum.

^cEnergy flux incident on the detector.

^dCorrected for absorption, and assuming a distance of 525 pc (Duerbeck 1981).

Table 2. Various model fits to the outburst spectrum.

	warm absorber	leaky absorber
More Absorbed Continuum		
norm. (10^{-2} photon $s^{-1}cm^{-2}keV^{-1}$)	7 ± 1	16 ± 13
temperature (keV)	> 43	15 ± 8
$\log N_H(cm^{-2})$	23.1 ± 0.2	24.3 ± 0.2
$\log N_{Fe}(cm^{-2})^b$	23.5 ± 0.2	24.3 ± 0.2^d
Less Absorbed Continuum		
norm. (10^{-2} photon $s^{-1}cm^{-2}keV^{-1}$)		7 ± 2
temperature (keV)		15 ± 8^c
$\log N_H(cm^{-2})$		23.0 ± 0.1
Iron Line		
line centre energy (keV)	6.7 ± 0.2	6.6 ± 0.2
line flux (10^{-4} photon $s^{-1}cm^{-2}$)	19 ± 7	23 ± 7
equivalent width (eV) ^c	450 ± 200	530 ± 400
χ^2/ν	1.34	1.16
degrees of freedom	28	27

^aQuoted errors refer to single-parameter 90 per cent confidence limits. For details of model description, see text.

^bIron column density converted into effective hydrogen column density, assuming cosmic iron abundance.

^cDefined with respect to the total continuum for the latter two models.

^dSet equal to N_H .

^eSet equal to the 'More Absorbed Continuum' temperature.

3.5 Rotational ephemeris of the white dwarf

We attempt to constrain the rotational ephemeris of the white dwarf in the GK Per system and its time derivative, if any, by combining our results in quiescence with other measurements. Before the *Ginga* observation, there were two *Einstein* observations (Eracleous, Patterson & Halpern 1991) and five *EXOSAT* observations (WKO85 for observations A-C, and NWK88 for observations D and E). In addition to these X-ray observations, three optical measurements (Patterson 1991), made after the *Ginga* observation, are available. There are, however, several problems in comparing the relative phasings of all the data due to differences in energy bands and/or in modulation patterns. Therefore, although the pulse arrival-time analysis is more sensitive for the present purpose, we have calculated average rotational periods from the arrival times of a couple of adjacent observations with similar source behaviour taken in similar energy bands. The average pulse-period history thus obtained is shown in Fig. 9, together with two lines indicating the constant period of 351.3410 s, and the constant \dot{P} of $-0.00082 s yr^{-1}$ after Patterson (1991). The constant \dot{P} line fits the data with χ^2 (d.o.f.) of 2.99(2). Though this value is formally unacceptable, it cannot be rejected in view of uncertainties in error estimation. One of the data points derived with the *EXOSAT* observation E and *Ginga* observation is nearly on the line, while the 'constant period' line is consistent with none of the cycle count aliases of the optical period. Therefore, if we include the optical period, the \dot{P} term is likely to exist. However, the detection of \dot{P}

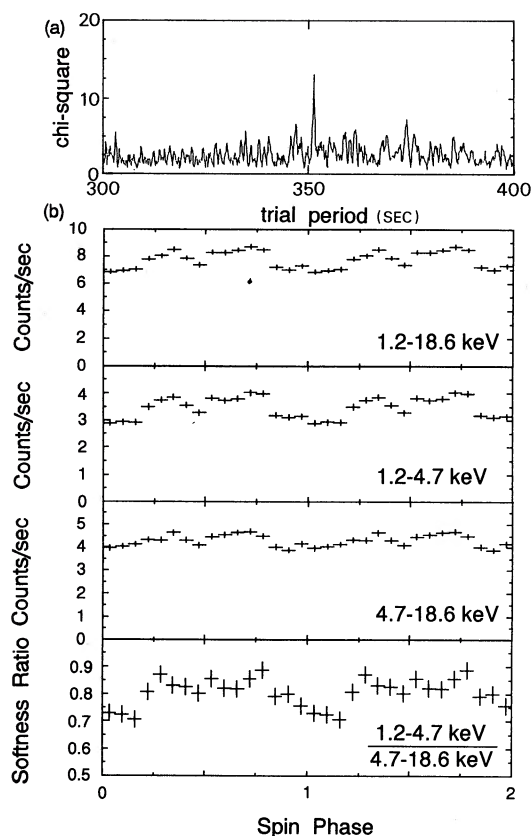


Figure 6. (a) Trace of the reduced chi-squared, from the standard epoch-folding analysis. (b) Background-subtracted X-ray modulation curves in several X-ray energy bands, together with the softness ratio, folded at a period of 351.3 s.

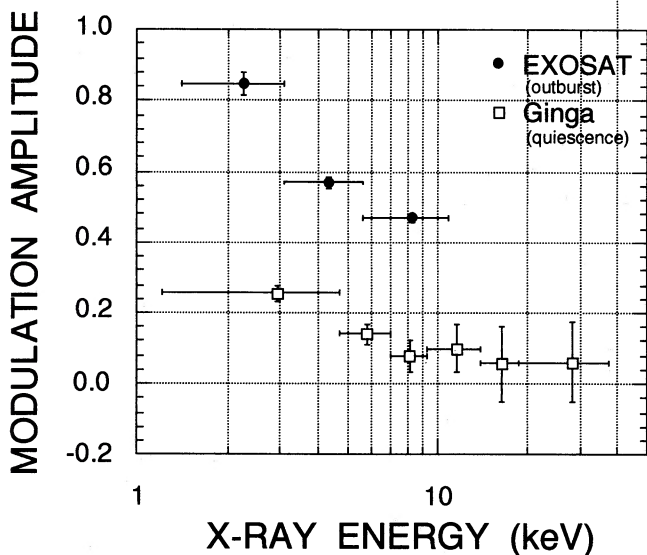


Figure 7. Energy dependence of the modulation amplitude (peak-to-peak amplitude divided by the maximum intensity) of GK Per in quiescence and in outburst. The outburst data are taken from WKO85.

should be regarded as tentative since, as Patterson (1991) mentioned, there is still ambiguity in the cycle counts. Further observations are necessary to establish the period change.

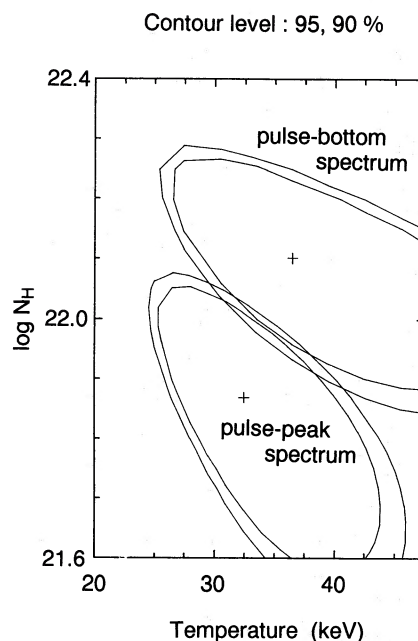


Figure 8. The confidence contours for the pulse-peak spectrum and the pulse-minimum spectrum in quiescence in the plane of kT and N_H . Contour levels are 95 and 90 per cent. The column densities are different at the 90 per cent confidence level.

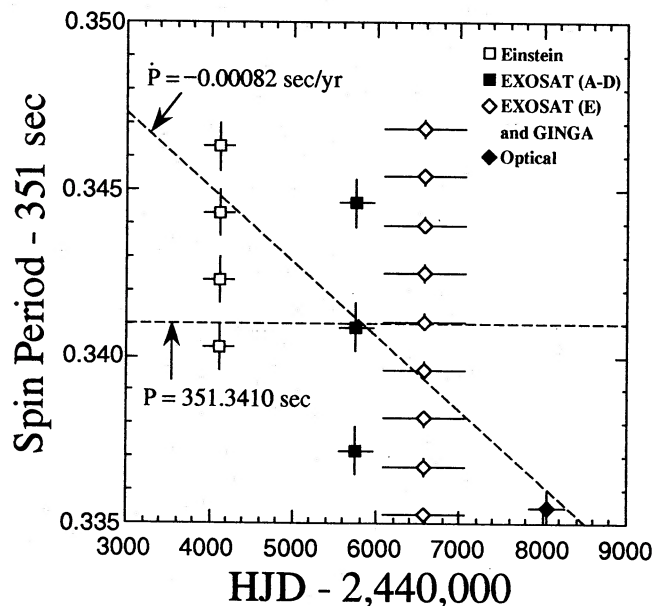


Figure 9. Pulse period history of GK Per. Horizontal bars show baselines to obtain average periods at each epoch. Best-fitting constant period line and constant \dot{P} line are shown together.

Assuming $\dot{P} = 0$ for simplicity we have attempted to refine the rotational ephemeris of the white dwarf in the GK Per system. For this purpose, however, we have to connect two sets of hard X-ray data in which the source behaviours are different, namely *EXOSAT* observations A-D (single-peaked modulation) and *EXOSAT* observation E-*Ginga* observation (double-peaked modulation). It seems reasonable to identify the deeper minimum of the *Ginga* light curve

with the minimum of the outburst light curve since the low-energy absorption in quiescence is largest at the deeper minimum (Fig. 6), which is also the case at the minimum in outburst (WKO85). The deeper minimum occurs at $HJD = 2447061.02165 \pm 0.00032$ in our data. Combining this timing with those obtained by WKO85 and NWK88, the mean times of the pulse minima are given as

$$T_{\min} = HJD\ 2445555.67592 + 0.0040664468E \\ (\pm 0.00011) \quad (\pm 0.0000000012)$$

4 DISCUSSION

4.1 Source behaviour in quiescence

In Table 3, we summarize the source behaviour in quiescence. The results of *EXOSAT* observations are quoted from NWK88. The current *Ginga* observation is consistent with observation E with respect to the source luminosity, pulse shape and the modulation amplitude. In particular, the *Ginga* data exhibit a double-peaked pulse profile which is similar to that of observation E. Thus the pulse profile may change from single peaked to double peaked when the 1–10 keV luminosity falls below $\sim 10^{33}$ erg s⁻¹, although the detailed mechanism is unclear.

Changes in the temperature as the luminosity varies are expected in simple models of the accretion column, as the height of the accretion shock is controlled by the accretion rate (Lamb 1985 and references therein). It is thus very important to clarify the relation between the luminosity and the temperature in order to understand the hard X-ray emission mechanism. From Table 3, the temperature seems substantially lower in observation E than in the *Ginga* observation, in spite of similar luminosities. However, we have reanalysed the data of observation E and obtained only a lower limit to the temperature of 34 keV. This reflects the difficulty of making accurate continuum measurements for weak hard sources with *EXOSAT*, and suggests that the errors quoted in NWK88 may have been underestimated. The *Ginga* light curve shows random intensity variations by a factor of ~ 3 (Fig. 1). We have sorted all the *Ginga* data into three groups according to the intensity level in the 1.2–18.6 keV band averaged over one spin period (< 10 , 10–15, and > 15 count s⁻¹), derived corresponding spectra, and fitted them with the single thermal bremsstrahlung model with absorption and the iron line. The resulting tem-

peratures cluster within a very narrow range of 29–33 keV with a typical error of 10 keV. Thus we conclude that there are no substantial variations in temperature in all the quiescence data taken with *EXOSAT* and *Ginga*. Higher quality spectra taken in a future outburst, especially covering the rise and the decline phases, would be of great value in further investigating this question.

4.2 Spectral parameters in outburst

The *Ginga* outburst spectrum is well explained by thermal bremsstrahlung provided that at least two different column densities are included in the model ($\sim 10^{23}$ and $\sim 10^{24}$ cm⁻²). WKO85 commented that the spectrum above ~ 4 keV could not be fitted with thermal bremsstrahlung. They concluded that a power law with energy index of ~ 0.5 could provide a good fit when combined with a soft excess model, in contradiction to the *Ginga* result. This discrepancy may not be so serious because, as pointed out by NWK88, the energy index of the outburst spectrum is about 0.4 if a leaky absorber model is adopted. This suggests that a high-temperature bremsstrahlung model might fit equally well, as this is the value of the energy index typical of bremsstrahlung in the energy range $E < kT$.

In Section 3.3 we tried to fit the observed outburst spectrum with various models. We found that the warm absorber model is somewhat inconsistent with observation, while the other three models are consistent with the data. Among them, the physical meaning of the soft excess model is unclear. WKO85 suggested that it may originate from the optically thin layer of the white dwarf. In the leaky absorber model, on the other hand, the two components can be understood as representing structure in the cold accretion column. We therefore feel that the leaky absorber model provides the most plausible interpretation of our outburst spectrum.

4.3 Modulation amplitude in quiescence and in outburst

We have shown in Section 3.4 that, in quiescence, the spin modulation of the light curve is mostly generated by variation in the column density. The light curves and softness modulation in outburst are qualitatively the same as those in quiescence (WKO85), suggesting the importance of the variation in column density for the spin modulation of the light curve in outburst also. In addition, both the average column density and the modulation amplitude are considerably larger in outburst (Table 1, Fig. 3, Fig. 7). These facts suggest that the low-energy absorption of GK Per originates from matter in the accretion column.

To discuss the accretion geometry in GK Per, however, we must relate the observed modulation curve to the geometrical spin phase. This is not trivial, for the relative importance of the absorption across and along the column varies with both the accretion rate and the fractional area of the column, even for a simple cylindrical accretion column (e.g. King & Shaviv 1984). To resolve this problem, it is essential to obtain evidence of occultation of the emission region by the white dwarf. Although there is no such evidence in the quiescence light curve, it is possible for occultation to play a substantial role in the spin modulation of outburst, for the Alfvén radius becomes smaller as the mass accretion rate increases. This is expected to increase the separation between the

Table 3. Source behaviour in quiescence.

	Observation D (<i>EXOSAT</i>)	Observation E (<i>EXOSAT</i>)	<i>GINGA</i>
Luminosity(1-10keV) ^a	1.4×10^{33}	8.9×10^{32}	7.3×10^{32}
Modulation amplitude ^b	21 ± 7	15 ± 4	14 ± 1
Pulse shape	single-peaked	double-peaked	double peaked
Temperature (keV)	33^{+95}_{-11}	$11^{+5}_{-3} (> 34)^c$	32^{+10}_{-7}

^aIn erg s⁻¹ assuming a distance of 525 pc.

^bPeak-to-peak amplitude in 2–6 keV divided by the peak intensity in units of per cent.

^cBased on the re-analysis.

emission region and the rotation axis of the white dwarf, and thus to increase the possibility of part of the emission region crossing the limb of the white dwarf, i.e. an occultation. Simple estimates demonstrate that this could be a significant effect: assuming the hydrogen number density of the accretion stream to be $\sim 10^{14}$ (Liebert & Stockman 1985) in quiescence, $\sim 10^{15}$ in outburst, and the magnetic moment of the white dwarf to be $\sim 10^{33}$ (all quantities are in cgs units), the colatitude of the emission region would vary 5° – 10° between quiescence and outburst for a $1-M_\odot$ white dwarf (see equations in Lamb 1985). Though the outburst pulse profile obtained with *EXOSAT* shows no feature that might be related to occultation, unless this feature is in phase with the absorption which produces most of the modulation, it may be worthwhile observing GK Per in outburst with a detector sensitive above 10 keV, in which energy band the effects of absorption and occultation can easily be separated.

Recently, Hellier and colleagues [e.g. Hellier, Cropper & Mason (1991) and references therein] have claimed that the absorption column density of intermediate polars is a maximum at the phase when we look down on the emission region along the accretion column, an idea based on measurements of the spin modulations of optical H and He line velocity. Such measurements may also help in clarifying the accretion geometry of GK Per.

5 CONCLUSION

We have found that the hard X-ray spectrum of GK Per in quiescence is well fitted by thermal bremsstrahlung with absorption and the iron line. The temperature is constrained to lie in the range 25–42 keV. The spectrum in outburst is also basically thermal, but much more absorbed than the quiescent spectrum and at least two components with substantially different column densities ($\sim 10^{23}$ and $\sim 10^{24}$ cm^{-2}) are needed. The difference in temperature between outburst and quiescence is not well constrained, due to the poor statistics of the outburst spectrum.

We have confirmed the 351-s spin modulation of the hard X-ray light curve during quiescence, and derived a more precise rotation ephemeris of GK Per. Evidence exists that the pulse-minimum spectrum is more absorbed than the pulse-maximum spectrum, and that low-energy absorption plays a crucial role in the spin modulation. The pulse profile in quiescence is more complex than that observed in the *EXOSAT* outburst observations, having two peaks per cycle. The origin of the change in the profile is not known, but might be related to the change in the accretion rate between outburst and quiescence, and hence to the accretion geometry.

It is important to observe the rise and the decline phases of the outburst, in order to investigate the relation between the luminosity and the temperature in magnetized cataclysmic variables and understand the accretion geometry which gives rise to the spin modulation of the light curve.

REFERENCES

- Becker, R. H. & Marshall, F. E., 1981. *Astrophys. J. Lett.*, **244**, L93.
 Cordova, F. A. & Mason, K. O., 1984. *Mon. Not. R. astr. Soc.*, **206**, 879.
 Crampton, D., Cowley, A. P. & Hutchings, J. B., 1983. In: *Cataclysmic Variables and Related Objects*, IAU Colloq. No. 72, p. 25, eds Livio, M. & Shaviv, G., Reidel, Dordrecht, Holland.
 Duerbeck, H. W., 1981. *Publs astr. Soc. Pacif.*, **93**, 165.
 Eracleous, M., Patterson, J. & Halpern, J. P., 1991. *Astrophys. J.*, **370**, 330.
 Hayashida, K. *et al.*, 1989. *Publs astr. Soc. Japan*, **41**, 373.
 Hellier, C., Cropper, M. & Mason, K. O., 1991. *Mon. Not. R. astr. Soc.*, **248**, 233.
 Hudec, R., 1981. *Bull. astr. Inst. Czech.*, **32**, 93.
 Illarionov, A. F. & Sunyaev, R. A., 1972. *Soviet Astr. A.J.*, **16**, 45.
 King, A. R. & Shaviv, G., 1984. *Mon. Not. R. astr. Soc.*, **211**, 883.
 King, A. R., Ricketts, M. J. & Warwick, R. S., 1979. *Mon. Not. R. astr. Soc.*, **197**, 77p.
 Kylafis, N. D. & Lamb, D. Q., 1979. *Astrophys. J. Lett.*, **228**, L105.
 Kylafis, N. D. & Lamb, D. Q., 1982. *Astrophys. J. Suppl.*, **48**, 239.
 Lamb, D. Q., 1985. In: *Low Mass X-ray Binaries and Cataclysmic Variables*, p. 179, eds Lamb, D. Q. & Patterson, J., Reidel, Dordrecht, Holland.
 Liebert, J. & Stockman, H. S., 1985. In: *Low Mass X-ray Binaries and Cataclysmic Variables*, p. 151, eds Lamb, D. Q. & Patterson, J., Reidel, Dordrecht, Holland.
 Morrison, R. & McCammon, D., 1983. *Astrophys. J.*, **270**, 119.
 Nagase, F., 1989. *Publs astr. Soc. Japan*, **41**, 1.
 Norton, A. J. & Watson, M. G., 1989. *Mon. Not. R. astr. Soc.*, **237**, 853.
 Norton, A. J., Watson, M. G. & King, A. R., 1988. *Mon. Not. R. astr. Soc.*, **231**, 789 (NWK88).
 Norton, A. J., Watson, M. G. & King, A. R., 1991. In: *Iron Line Diagnostics in X-ray Sources*, ed. Treves, A., Springer, in press.
 Norton, A. J., Watson, M. G., King, A. R., McHardy, I. M. & Lehto, H., 1990. In: *Accretion-Powered Compact Binaries*, p. 209, ed. Mauche, C. W., Cambridge University Press, Cambridge.
 Patterson, J., 1991. Preprint.
 Pounds, K. A., Nandra, K., Stewart, G. C., George, I. M. & Fabian, A. C., 1990. *Nature*, **344**, 132.
 Turner, M. J. L. *et al.* 1989. *Publs astr. Soc. Japan*, **41**, 345.
 Warner, B., 1976. In: *Structure and Evolution of Close Binary Systems*, IAU Symp. No. 73, p. 85, eds Eggleton, P., Mitton, S. & Whelan, J., Reidel, Dordrecht, Holland.
 Watson, M. G., King, A. R. & Osborne, J. P., 1985. *Mon. Not. R. astr. Soc.*, **212**, 917 (WKO85).